JOURNAL OF SPACECRAFT AND ROCKETS
Vol. 29, No. 5, September–October 1992

Solar Absorptance Degradation of Optical Solar Reflector Radiators on the SPACENET Satellites

Charles R. Naegeli*
GTE Spacenet Corporation, McLean, Virginia 22101

The subject of thermophysical property degradation of spacecraft materials has been a concern of thermal engineers for decades. A limited amount of on-orbit flight experience for spacecraft radiator's solar absorptance increases has been published. This paper describes the solar absorptance increases calculated for the fused silica optical solar reflectors on the SPACENET I and SPACENET II satellites. Comparison of these results with previously published results on other satellites is also made. Variation of results between satellite programs, however, indicate that other design elements and not the properties of the optical solar reflector itself contribute to this degradation. In particular, the processes of photolysis or the photochemical reactions induced by solar vacuum ultraviolet radiation on spacecraft contaminants is tested and supported by this analysis. This is accomplished through the separation of long-term temperature trends based on sunlit and nonsunlit periods. The methods employed in this analysis are primarily statistical manipulations on a large data base. This is required since the time constant is of the order of years, and discrete thermal reduction techniques are prone to error and uncertainty due to the thermal dissipation distribution associated with the operation of the satellite. The classical approach to time series analysis using a moving average model that is presented is graphically and measurably accurate to a high degree.

Nomenclature

K	= sensitivity of $dT/d\bar{Q}_{inc}$ to changes in α_s
$\bar{Q}_{abs}$	= mean seasonal solar absorbed flux, W/m^2
$\bar{Q}_{inc}$	= mean seasonal solar incident flux, W/m^2
$\bar{Q}_{sol}$	= solar incident flux at solstice, W/m^2
r	= correlation coefficient
t	= time (days in sunlight)
t_0	= initial time
α_s	= solar absorptance
$\bar{\alpha}_s$	= mean of mission of α_s
δT	= temperature rise, °C
$\bar{\delta T}$	= mean temperature rise, °C
δT_{max}	= maximum temperature rise, °C
σ	= standard error, °Φ
τ	= time constant

Introduction

SPACENET I and II satellites are communications hybrids carrying a payload of 24 transponders, 12 narrow-band C solid state power amplifiers (SSPA), and 6 wideband C traveling wave tube assemblies (TWTA), in addition to 6 Ku-band TWTAs. The satellites were built by GE Astro Space Division, and their design heritage is of the early SATCOM satellites. SPACENET I was launched in May of 1984 followed by SPACENET II in November of 1984, they are three-axis stabilized and on station in the geosynchronous arc.

The SPACENET satellite is shown in Fig. 1. The predominant dc dissipation components are the TWTAs, which are located on the south panel, and the SSPAs, which are located on the north panel. The major portion of the rf output power of these components is radiated through antennas located on the Earth-pointing side of the satellite, although a significant amount of thermal loss occurs through passive components such as waveguides, output multiplexers, and power dividers in the core of the satellite and on the panel beneath the antennas.

The thermal control system is passive with heater augmentation. The major heat rejection path is through radiators located on the north and south panels. The radiators consist of individual optical solar reflectors (OSR) that are bonded to an aluminum honeycomb substate. The OSR is a fused silica second surface mirror manufactured by Corning. Heat sinks are utilized to spread the dc losses from the TWTAs and SSPAs to the radiator panels. With minor differences, the thermal design of both satellites is identical.

It is the degradation of the solar absorptance α_s of the OSR that is responsible for the general warming of the spacecraft over time. The degradation is influenced by spacecraft contamination (e.g., outgassing of organic molecules) in the presence of sunlight. Results of this study for SPACENET I and II are shown in Fig. 2 as a comparison to previously published alpha degradation rates exhibited by satellite radiators. [This is a figure prepared by Gluck[1] to which data from Defense Satellite Program (DSP) Flight 10, Satellite Data System (SDS), and Defense Satellite Communication System (DSCS) III were added by Hall et al.[2]. SPACENET I and II south radiator panels were added by the author.]

Research performed at the Aerospace Corporation, among others, describes the ground-based testing and theories associated with the degradation process.[2–4] This research serves mainly to test and support the hypothesis that the degradation occurs only under the catalytic activity of direct sunlight. The degradation for SPACENET I and II is shown as a continuous curve (to compare with the other satellite programs), but in reality, the degradation process stops or slows significantly during non-sunlit periods. A more accurate accounting of the degradation process was to plot temperature rise and degradation rates as a function of time in sunlight. The methods employed in the determination of the alpha degradation curve fit is the subject of the remainder of this paper.

Thermal Model

The thermal model originally developed at the time of the critical design review was regenerated from input data and used to correlate the on-orbit results with the model predic-

Received June 2, 1990; presented as Paper 90-1671 at the AIAA/ASME 5th Joint Thermophysics and Heat Transfer Conference, Seattle, WA, June 18–20, 1990; revision received Feb. 12, 1991; accepted for publication May 1, 1991.

*Supervisor, Flight Operations Engineering, Engineering and Development, 1700 Old Meadow Road; currently, Optical Telescope/Payload Manager, Hubble Space Telescope Ground System and Operations Project, Flight Projects Directorate, NASA Goddard Space Flight Center, Greenbelt, MD, 20771. Member AIAA.

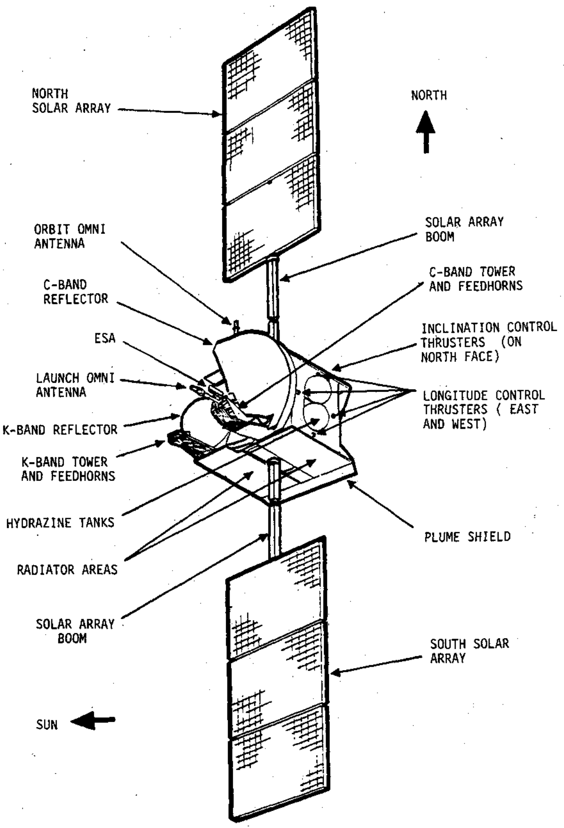

Fig. 1 SPACENET satellite.

tions. Results of this study were provided in detail by the author previously,[5] and it is his only intention here of summarizing some of the conclusions drawn from this study as it relates to the long-term temperature rise and associated degradation of the OSRs.

The thermal model, for instance, was helpful in determining the temperature sensitivity of the satellite components to varying on-orbit electrical dissipations. Knowledge of the boundary conditions that define the thermal model output is imperative in establishing a high-confidence level in the accuracy of the results of a study of this nature and is cited in the literature as a limiting factor in the determination of the solar absorptance degradation of the OSR.[6,7] The determination of the electrical state was reduced from spacecraft telemetry. It must be noted that reduction of actual telemetry data under the range of possible satellite operational configurations is an inexact procedure. The approach taken by the author was to improve the data base of raw telemetry data (i.e., normalize the data) and then through the examination of a large volume of data reduce the random thermal error. The reader may find it useful to review what was for the author the most exhaustive part of the study; however, ultimately, it is the statistics that lend the greatest credibility to the results and observations that are made herein, (i.e., a necessary evil).

The temperature output of the thermal model for the diurnal cases of equinox and solstices, as well as successive weekly steady-state cases, was also compared to the normalized thermistor data gathered for the empirical study. This exercise made it possible to draw some general conclusions regarding the accuracy of the thermal model and to correlate any deviations from predictions to the incident solar flux to the radiator panels. For example, although many of the components differed significantly from predictions, the error between prediction and actual was nearly constant throughout the year and not what one would have expected if there was a relationship to solar flux on either the north or south panels. However, examination of the deviations from the diurnal and yearly cases did show a strong correlation to incident flux at the aft end of the spacecraft in the area of the apogee kick motor (AKM). This indicated an unaccounted for heat source in this region. Moreover, those components that were most coupled to the radiator panels (e.g., the TWTAs and SSPAs) showed only marginal deviation from prediction.

Of the two components identified as being overly influenced by incident flux to the south panels, only the command receiver located on the antenna panel is included in this study. In this case, although the empirical results of the long-term temperature trend were consistent with the other components, the thermal model was unreliable in describing the temperature sensitivity to absorbed solar flux. This precluded the use of this component in making an absolute determination of OSR solar absorptance degradation. In general, it can be stated that the thermal model was inaccurate insofar as absolute temperature comparisons were made, but sufficiently accurate to make the temperature sensitivity to absorbed flux calculations necessary to arrive at an absolute α_s value.

Figure 3 profiles the command receiver thermal response, which is used as an example of a sample component included in the data base. What is plotted here is the normalized mean daily temperature as a function of day of year. The normalized data base reduces the raw telemetry data to a condition of constant satellite electrical state and configuration. Successive years (through 1989) are plotted parametrically in the scatter diagram. The normalized temperature data for a few geographically distributed components were used as a basis for all subsequent analysis.

Empirical Model

The empirical model was created from the normalized data base of successive Sunday mean telemetry data and consisted of 290 cases for SPACENET I and 267 cases for SPACENET II. Sunday was chosen for the case study because command

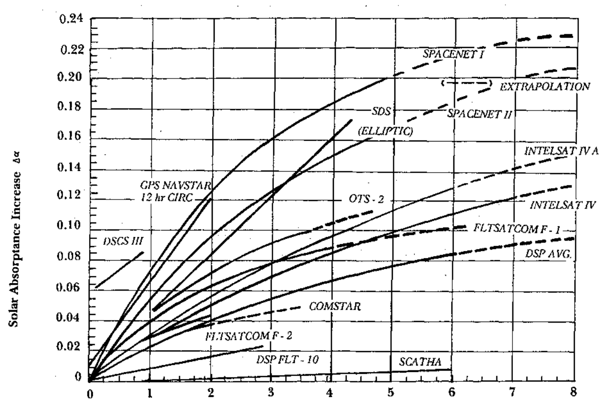

Fig. 2 Degradation of several silverized fused silica second surface mirrors vs time.

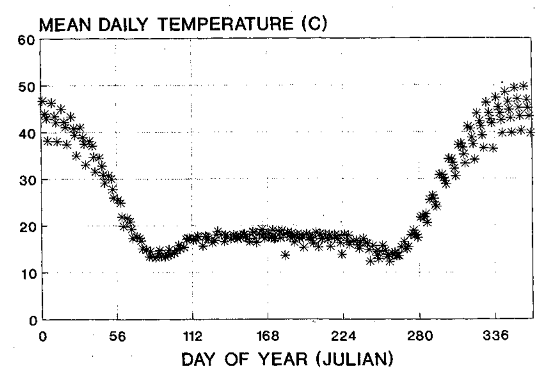

Fig. 3 Normalized mean daily temperature of the SPACENET I command receiver.

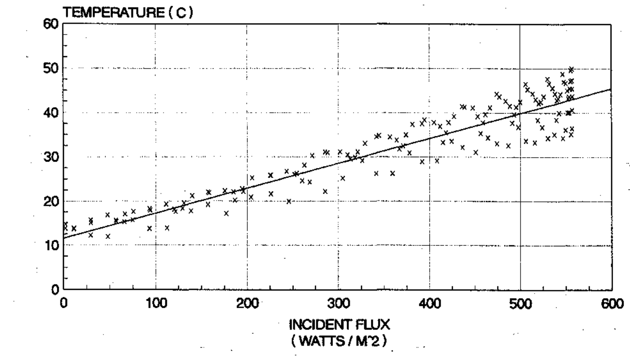

Fig. 4 Simple linear regression of command receiver normalized temperature vs solar incident flux.

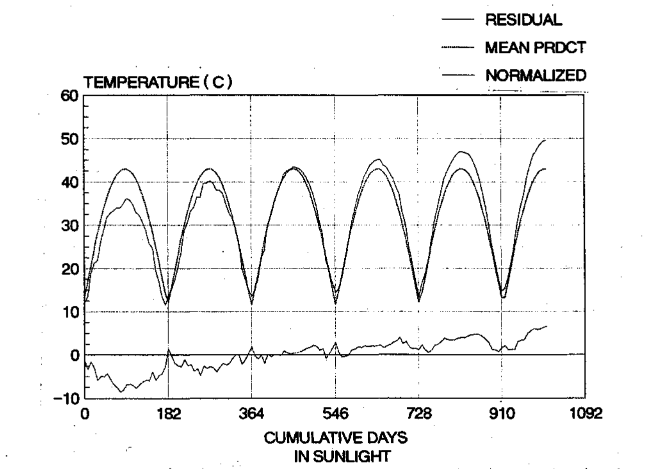

Fig. 5 Mission mean temperature profile of command receiver and calculated temperature residuals.

and transponder activity is minimal on that day and the satellite would have had ample time to recover from any transient effects associated with maneuvers during the latter part of the work week. In order to separate the effects of solar absorptance degradation of the north and south OSR panels, this data base was further divided into two subsets: 1) summer seasonal: solar flux incident to the north panel (26 weeks from vernal to autumnal equinox); and 2) winter seasonal: solar flux incident to the south panel (26 weeks from autumnal to vernal equinox). Each subset was inclusive of the entire record of the satellites from launch. The eight nodal locations (not shown) chosen for the study had a strong temperature dependance on the solar input to the radiator panel. Results of the statistical analysis for each of the components correlated to a panel were consistent one with the other; however a weighted average was used to summarize the cumulative effect on the satellite. The weights were based on relative coupling to the OSR radiator panels.

A simple linear regression of the thermal data as a function of incident flux to the radiator panel was performed. A theoretical mission mean temperature profile was obtained to which the normalized temperature data for successive years was compared. This methodology proved to be more accurate than just calculating the temperature differences from a preceding year. The regression procedure reduces the residual thermal error from the normalization process as well as the granularity of the telemetry data itself. For the purpose of this study, all temperature differences were reduced from the theoretical mission mean profile. Figures 4 and 5 graphically describe the calculation of the temperature residuals for the command receiver on SPACENET I during the winter seasonal period.

In order to eliminate the problem of having a common set of environmental boundary conditions of which to fit a curve describing the long-term temperature trend, the data base of temperature residuals was transformed into a moving average of 26 successive weeks that defined the mean temperature residual for the moving season. The moving season does not, of course, correspond to any specific interval of time but rather the continuous cyclical pattern of the solar vector. Successive data points drop one residual and add one residual to the average during the stream of time. Consequently, a large number of data points were obtained (e.g., 120 each for the summer and winter seasonal periods for SPACENET I). Figures 6–9, respectively, show the comparison between the temperature residuals at a point in time and the moving average for the command receiver and the weighted average of components (both winter and summer seasons and both spacecraft are represented). A constant equivalent to the mean of the moving average of the residuals over the mission to date $\bar{\delta T}$ is added to the dependent variable. This transformation shifts the curve upward so that the y-axis intercept is at day 182 (the initial value).

The moving average trend is smooth and lends itself to reduction by a number of different equational forms. Many of them, including a linear form, can be shown to have a high correlation with the data (since it is nearly linear over the time span). The inverse exponential equation [Eq. (1)] was found to fit the data with the highest correlation coefficient (≥ 0.957) and also was bounded at day = 182, $\delta T \approx 0$ and at day = ∞, $\delta T = \delta T$max (the asymptotic value).

The form of this equation is

$$\delta T = \delta T_{\max} * \{1 - e^{-(t-t_0)/\tau}\} \tag{1}$$

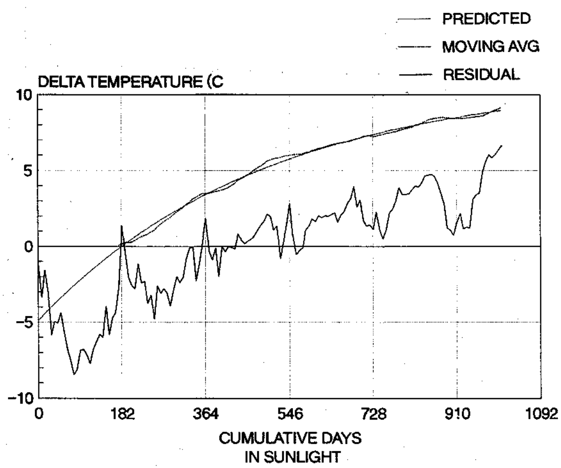

Fig. 6 SPACENET I command receiver long-term temperature trend during winter seasonal period.

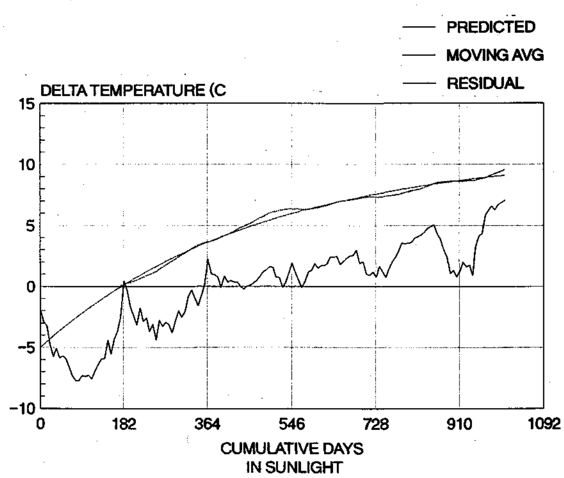

Fig. 7 Weighted average of components' long-term temperature trend: SPACENET I, winter seasonal period.

Table 1 Coefficients for exponential fitting of moving average trend

Satellite	Season	Component	δT_{max}, °C	τ	$\delta\bar{T}$, °C	r	σ, °C	$(\delta\alpha_s/\bar{\alpha}_s)\vert_{max}$
S-I	Winter	Command receiver	11.0	492.6	5.5	0.997	0.04	
S-I	Winter	Weighted average	10.9	471.7	5.7	0.992	0.06	0.744
S-I	Summer	Weighted average	9.8	769.2	3.8	0.985	0.06	0.977
S-II	Winter	Weighted average	10.8	632.9	3.7	0.957	0.11	0.728

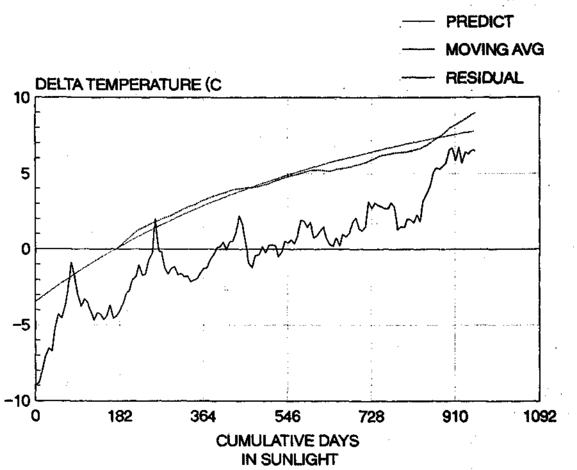

Fig. 8 Weighted average of components' long-term temperature trend: SPACENET II, winter seasonal period.

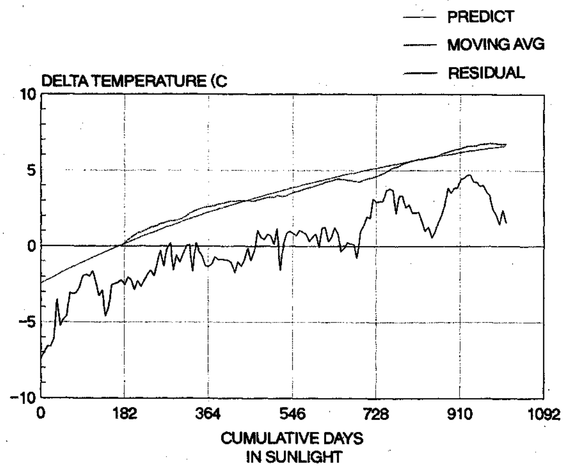

Fig. 9 Weighted average of components' long-term temperature trend: SPACENET I, summer seasonal period.

The constant $t_0 = 182$ to correspond to the initial value of this data base. This equation was described in the publication of the thermal results of the first European telecommunications spacecraft Orbital Test Satellite (OTS-2) after six years in orbit.[8] The form of this equation is described as fitting previous experimental degradation data obtained in laboratory tests.[9]

A direct solution to the coefficients of Eq. (1) is not obtainable, but may be obtained by transformation of the variable δT to the more manageable $(\delta T_{max} - \delta T)$. Without foreknowledge of the constant δT_{max}, a solution could only be arrived at through an iterative process and only if the initial and final boundary condition could be met (i.e., $\delta T = 0$ at $t = 182$, and $\delta T = \delta T_{max}$ at $t = \infty$). Since δT_{max} is assumed in the form of the variable, the solution to the coefficient is bound to one and only one value.

Fortunately, a solution was obtained that met all of the constraints imposed on it (Figs. 6–9). The coefficients of Eq. (1) are provided in Table 1 as well as the correlation coefficients r and standard errors σ to the moving average trends. The overall accuracy of the curve fitting routine is 0.11°C or less than the accuracy of an individual thermistor measurement.

Since δT, as calculated, represents the seasonal average rise, the peak seasonal temperature rise is equal to the ratio of the maximum solar incident flux (at solstice) to the mean seasonal solar incident flux times δT:

$$\begin{aligned}\delta T_{max} &= (Q_{sol}/\bar{Q}_{inc})^*\delta T \\ &= 1.58^*\delta T \quad \text{(at winter solstice)} \\ &= 1.51^*\delta T \quad \text{(at summer solstice)}\end{aligned} \tag{2}$$

Comparison of the coefficients of this work with those from the OTS-2 study is not readily done since the author chose a moving average as the test variable while Bouchez and Howle[8] examined only solstice and equinox conditions. The other notable difference between studies is that time in this study is only during sunlit conditions (e.g., 1/2 year), whereas it appears that the clock counts continuously from launch in their study. The time constant τ is roughly the same value in both studies after adjusting for the differences between the time variable. Since the thermal sensitivity to α_s would be different between satellites, a comparison of δT_{max} would be meaningless.

Thermal Degradation of the Optical Solar Reflector

The degradation of the solar absorptance α_s of the OSR is the predominant contributor to the increase in the satellite component temperatures over time since all of the other thermal variables were accounted for and none had shown a long-term correlation with time. A measure of this degradation can be calculated based solely on empirical data since the solar incident flux to the radiator panels is known with a high certainty. The measure, however, falls short of defining an initial value, a mean value, or, for that matter, a value at any point in time. Nonetheless, the following derivation of α_s is offered. The formulation is exact and is dependent only on the derivation of $\overline{\delta T/\delta Q_{inc}}$, which is obtained from a linear regression of the normalized data (see Fig. 4). Since $\delta\alpha_s$ is calculated based on the moving average, $\delta\alpha_s$ as computed lags time by 91 days; α_s is constant during nonsunlit periods (apparent from inspection of the normalized curves)

$$\begin{aligned}\delta\alpha_s/\bar{\alpha}_s &= \delta T/(\bar{\alpha}_s{}^*\overline{\delta T/\delta\sigma_s}) \\ &= \delta T/(\overline{\delta T/\delta Q_{inc}}{}^*\delta\bar{Q}_{abs}/\alpha_s)\end{aligned}$$

where (3)

$$\begin{aligned}\delta\bar{Q}_{inc} &= \delta\bar{Q}_{abs}/\alpha_s \\ \delta\bar{Q}_{abs}/\delta\alpha_s &= 352\ \text{W/m}^2 \text{ at winter seasonal} \\ &= 344\ \text{W/m}^2 \text{ at summer seasonal}\end{aligned}$$

Figures 10 and 11 show the computed values of $\delta\alpha_s$ as a comparison between north to south radiator panels for SPACENET I, and also between satellites for the south panel.

An estimate of the mission mean $\bar{\alpha}_s$ was necessary to complete the analysis. The thermal model was used for this purpose. Solution to $\bar{\alpha}_s$ was made by fitting the slope of the temperature vs incident flux curve to its sensitivity to solar absorptance. This was derived by exercising the thermal model parametrically for α_s. In Eq. (4), δ refers to the delta operator as derived from the empirical data and d to the delta operator obtained from the thermal model. By fitting the data to a gradient, the errors associated with absolute temperature compar-

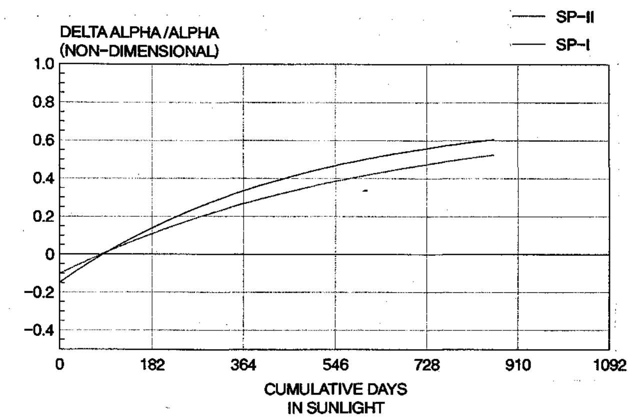

Fig. 10 Empirical measurement of OSR solar absorptance degradation: SPACENET I and II south radiators.

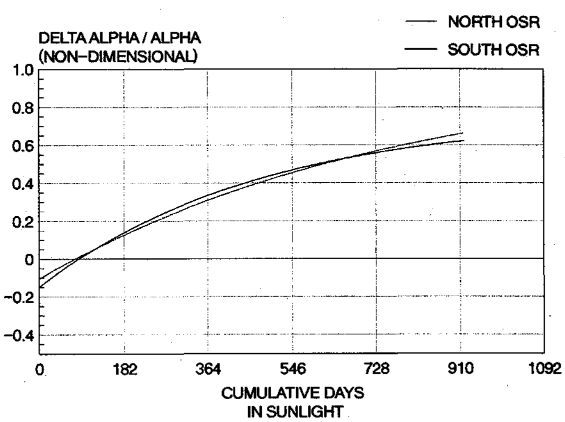

Fig. 11 Empirical measurement of OSR solar absorptance degradation: SPACENET I, north and south radiators.

isons are effectively removed. Thus, any deviations from predictions associated with flux to any of the other satellite external surfaces do not contribute to an error in the estimation of α_s. As mentioned earlier, the error between prediction and actual for the command receiver showed a strong correlation to incident flux to the radiator panel. This component data was removed from the solution of the absolute determination of α_s.

$$\bar{\alpha}_s = 0.25 + \{\overline{\delta T/\delta Q_{\text{inc}}} - dT/dQ_{\text{inc}}|_{\alpha=0.25}\}/K \qquad (4)$$

where

$$K = d[\mathrm{d}T/dQ_{\text{inc}}]/d\alpha_s$$

For SPACENET I and II, the mean solar absorptance was 0.26. This would correspond to its value at approximately three years in orbit and would be consistent with an initial value of about 0.10 at launch. Note that the long-term trend is projected forward from day 91. The absolute solar absorptance curves that were presented in Fig. 2 are, in addition, extrapolated backward to day 0.

Definitive explanations for the slight variation among these curves can not be offered and may be statistically insignificant. However, it seems likely that the higher rate of degradation of SPACENET I is attributed to a larger volume of satellite contamination since increasing cleanliness procedures were implemented during the series development.

Conclusions

Telemetry data on SPACENET I and SPACENET II were gathered in order to determine the long-term temperature trend and associated solar absorptance degradation of the optical solar reflectors. The OSRs, which are silverized fused silica second surface mirrors, are the primary satellite radiators. Separation of the data into sunlit and nonsunlit periods allowed the author to confirm the hypothesis that degradation occurs under the catalytic activity of direct sunlight on spacecraft contaminants.

An inverse exponential curve fit to the empirical thermal data showed a high correlation and small standard errors. The empirical data alone was used to determine the long-term temperature rise and to calculate a measure of the solar absorptance degradation. The thermal model, however, was necessary to calculate the thermal sensitivity of various components to changes in the solar absorptance and to make an absolute determination of α_s. The slight differences between degradation rates between SPACENET I and SPACENET II satellites is thought to be related to the volume of spacecraft contaminants. Contamination accretion rates have been indicated to be the dominant factor associated with the wide variation in alpha degradation rates among satellites in previously published reports.

Acknowledgment

The author wishes to thank GE Astro Space Division for the use of the illustration and for the input data for the thermal model generation.

References

[1]Gluck, D., private communication, Oct. 1983.

[2]Hall, D. F., Stewart, T. B., and Hayes, R. R., "Photo-Enhanced Spacecraft Contamination Deposition," AIAA Paper 85-0953, June 1985.

[3]Stewart, T. B., Arnold, G. S., Hall, D. F., Marvin, D. C., Hwang, W. C., Chandler, R. D., Marten, H. D., "Photochemical Spacecraft Self Contamination: Laboratory Results and Systems Impacts," AIAA Paper 88-2728, June 1988.

[4]Ahern, J. E., Belcher, R. L., and Ruff, R. D., "Analysis of Contamination Degradation of Thermal Control Surfaces in Operational Satellites," AIAA Paper 83-1449, June 1983.

[5]Naegeli, C. R., "Spacenet I, II 5 Years in Orbit—Review of the Thermal Trends Observable in a Passive Thermal Design of Two Communication Satellites," AIAA Paper 90-1671, June 1990.

[6]Bouchez, J., and Gulpen J., "The European Geostationary Communication Satellite OTS—Two Years of Thermal Control Experience in Orbit," AIAA Paper 80-1500, June 1980.

[7]Chalmers, D., "Solar Absorptance Degradation of OSR Radiators on European Communication Satellites," AIAA Paper 84-1700, June 1984.

[8]Bouchez, J., and Howle, D., "OTS-2; Results from Thermal Tests on a Satellite During Six Years in a Geostationary Orbit," AIAA Paper 84-1701, June 1984.

[9]Paillous, A., "Qualification des Revetements de Controle Thermique aux Rayonnements Ultraviolets et Particulaires de l'Espace," ONERA × DERTS, Doc. 29/4025/TS, Juliet, France, 1975.

Alfred L. Vampola
Associate Editor